patients with severe hemolytic jaundice and high copper, but many countries have limited use of chelation therapy to late childhood and adulthood. α-Tocopherol or other antioxidants may be administrated as usual *(25)*.

We are highly indebted to Anna Stamatis for assistance with the preparation of this manuscript and to Maria Papastamatakis for excellent technical assistance.

References

1. Ostermeier C, Iwata S, Michel H. Cytochrome c oxidase. Curr Opin Struct Biol 1996;6:460–6.
2. Sullivan JL, Ochs HD. Copper deficiency and the immune system. Lancet 1978;2:686.
3. Vyas D, Chandra RK. Thymic factor activity, lymphocyte stimulation response and antibody producing cells in copper deficiency. Nutr Res 1983;3:343–50.
4. Araya M, Koletzko B, Uauy R. Copper deficiency and excess in infancy: developing a research agenda. J Pediatr Gastroenterol Nutr 2003;37: 422–9.
5. Widdowson E. Trace elements in fetal and early postnatal development. Proc Nutr Soc 1974;33:275–84.
6. Al-Rashid RA, Sprangler J. Neonatal copper deficiency. N Engl J Med 1971;285:841–3.
7. Ashkenazi AS, Levin S, Djaldetti M, Fisher E, Benvestini D. The syndrome of neonatal copper deficiency. Pediatrics 1973;52:523–33.
8. William DM. Copper deficiency in humans. Semin Hematol 1983;20:118–28.
9. Cizewski-Culuta V, Gitlin JD. Disorders of copper transport. In: Scriver CR, Beaudet AL, Sly WS, eds. Metabolic and molecular bases of inherited disease, 8th ed. New York: McGraw-Hill, 2000:3105–28.
10. Hannam S, McDonnell M, Rennie IM. Investigation of prolonged neonatal jaundice. Acta Pediatr 2000;89:694–7.
11. Maisel JM. Jaundice in neonatology. In: Avery GB, Fletcher MA, McDonald MG, eds. Pathophysiology and management of the newborn, 4th ed. Philadelphia: JB Lippincott, 1994:630–60.
12. Henry RJ, Chiamoris N, Jacobs SL, Seaglove M. Determination of ceruloplasmin oxidase activity in serum. Proc Soc Exp Med Biol 1960;104:620–4.
13. Terres-Martos C, Navarro-Alarcon M, Martin-Lagos F, Lopez-Carcia de la Serrana H, Lopez Martinez MC. Determination of Cu levels in serum of healthy subjects by atomic absorption spectrometry. Sci Total Environ 1997;198:97–103.
14. Bremer J. Manifestations of copper excess. Am J Clin Nutr 1998;67(Suppl): 1069–73.
15. Fuentealba C, Aburto EM. Animal models of copper-associated liver disease. Comp Hepatol 2003;2:1–12.
16. Valaes T, Karaklis A, Stavrakakis D, Bavela-Stavrakakis K, Perakis A, Doxiadis SP. Incidence and mechanism of neonatal jaundice related to glucose-6-phosphate dehydrogenase deficiency. Pediatr Res 1969;3:448–58.
17. Kaplan M, Beutler E, Vreman HJ, Hammerman C, Levy-Lahad E, Renbau P, et al. Neonatal hyperbilirubinemia in G6PD deficient heterozygotes. Pediatrics 1999;104:68–74.
18. Rossipal E, Krachler M, Li F, Micetic-Turk D. Investigation of the transport of trace elements across barriers in humans: studies of placental and mammary transfer. Acta Paediatr 2000;89:1190–5.
19. Chen BH, Tsai JL, Tsai LY, Chao MC. Comparison of serum copper, magnesium, zinc and calcium levels between G6PD deficient and normal Chinese adults. Kaohsiung J Med Sci 1999;15:646–50.
20. Schilsky ML, Scheinberg IH, Sternlieb I. Liver transplantation for Wilson disease. Indications and outcome. Hepatology 1994;19:583–7.
21. Strand S, Hofmann WS, Grambihler A, Hug H, Volkmann M, Otto G, et al. Hepatic failure and liver cell damage in acute Wilson's disease involve CD 95 (Apo-I/Fas) mediated apoptosis. Nat Med 1998;4:588–93.
22. Suzuki KT, Shiobara Y, Tachibana A, Ogra Y, Matsumoto K. Copper increases in both plasma and red cells at the onset of acute hepatitis. Res Commun Mol Pathol Pharmacol 1999;103:189–94.
23. Sokol RJ. Antioxidant defenses in metal induced liver damage. Semin Liver Dis 1996;16:39–46.
24. Fridovich J. Superoxide anion radical superoxide dismutases and related matters. J Biol Chem 1997;272:515–7.
25. Sokol RJ, McKim JM, Devereau MW. α-Tocopherol ameliorates oxidant injury of isolated copper overloaded rat hepatocytes. Am J Clin Nutr 1998; 67(Suppl):1012–6.
26. Fridovich J. Superoxide radical and superoxide dismutases. Annu Rev Biochem 1995;64:97–112.
27. Van Wassenaer-van Hall HN. Neuroimaging in Wilson's disease. Metab Brain Dis 1996;12:1–19.

DOI: 10.1373/clinchem.2004.031773

Trehalose Is a Potent PCR Enhancer: Lowering of DNA Melting Temperature and Thermal Stabilization of *Taq* Polymerase by the Disaccharide Trehalose, *Andrej-Nikolai Spiess,* Nadine Mueller, and Richard Ivell* (Institute for Hormone and Fertility Research, Centre of Innovative Medicine, Falkenried 88, 20251 Hamburg, Germany; * author for correspondence: fax 49-40-42803-1699)

Compatible solutes are a class of compounds that stabilize cells and cellular components exposed to extreme conditions. In bacterial systems, the uptake or synthesis of compatible solutes renders the cells and their enzymatic machinery more resistant to stress-inducing environmental conditions such as high osmolarity or high temperatures *(1, 2)*. Compatible solutes comprise a heterogeneous group of compounds, covering amino acids and their derivatives *(3)*, sugars *(4)*, and more obscure compounds such as the pyrimidine derivative ectoine *(5)*.

The compatible solute trehalose is a nonreducing disaccharide in which two D-glucose units are linked by an α,α-1,1-glycosidic bond. It is synthesized by a variety of eukaryotic organisms, conferring tolerance against desiccation, dehydration, heat, cold, and oxidation *(6)*. The addition of trehalose increases the enzymatic activity of several euthermal enzymes used for cDNA synthesis or restriction digestion of DNA *(7, 8)*. Trehalose also enhances the priming specificity in differential-display reverse transcription-PCR *(9)* through high-temperature priming and a thermoactivated reverse transcriptase.

PCR amplifications are frequently impaired by high GC content of the target sequence, leading to low yield and specificity of products, with no product at all in the worst cases. Locally high-temperature melting regions within the template can act as permanent termination sites *(10)*. Several low-molecular-weight products have been identified that enhance the PCR of difficult templates, e.g., dimethyl sulfoxide *(11)* and other sulfoxides *(12)*, formamide *(13)*, nonionic detergents *(14)*, and compounds belonging to the family of compatible solutes, such as betaine *(15–17)*. The latter is present in most of the commercially available PCR-enhancing solutions *(18)*.

Here we report the application of trehalose as a potent PCR enhancer for GC-rich templates. This compound avoids false negatives in PCR typing *(16)*. In this study, we used trehalose in real-time, reverse transcription-PCR amplification of the mouse oxytocin receptor (mOT-R) transcript, which has a very high GC content. The identified molecular properties of this compound that lead to its PCR-enhancing ability are based on (*a*) lowering the melting temperature of DNA and (*b*) thermostabilization of the *Taq* polymerase.

Total RNA was prepared from 100 mg of mouse brain

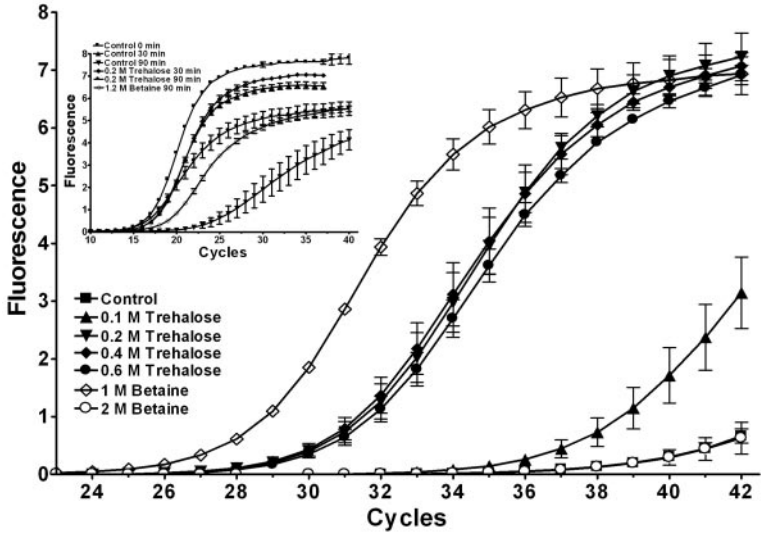

Fig. 1. Real-time amplification of the mOT-R transcript with increasing concentrations of trehalose and betaine as a comparison and of S27a after thermal stressing of the *Taq* polymerase in the presence of trehalose and betaine.

Shown is the amplification curve from the real-time PCR of mOT-R with increasing concentrations of trehalose and the commonly used PCR additive betaine in the PCR cocktail. The *inset* shows the amplification curves of a S27a real-time PCR reaction with *Taq* polymerase that had been thermally stressed for 30 and 90 min in the absence or presence of trehalose and betaine before its use in the PCR reaction. *Error bars*, SD.

tissue by use of the RNeasy™ Mini Kit (Qiagen) according to the manufacturer's protocol. cDNA synthesis was conducted according to the manufacturer's protocol (Superscript™; Invitrogen). Real-time PCRs were conducted with reagents as described *(19)* but adding various concentrations of D-(+)-trehalose (Sigma T-5251) in a total volume of 20 μL. Primers specific for mOT-R were mOT-R sense (5′-ttctacgggcccgacctgctgtgt-3′) and mOT-R antisense (5′-ctgtgcggattttggccttggaga-3′; product size, 492 bp; positions 877-1368 of GenBank accession no. D86599), and those for the mouse ribosomal protein S27a were S27a sense (5′-ccaggataaggaaggaattcctcctg-3′) and S27a antisense (5′-ccagcaccacattcatcagaagg-3′; product size, 296 bp; positions 117–413 of GenBank accession no. BC002108). Initial denaturation was for 3 min at 95 °C to activate the enzyme, after which 30–50 cycles of amplification were performed with denaturation at 95 °C for 30 s, annealing at primer-specific temperatures (mOT-R, 68 °C; S27a, 60 °C) for 10 s, and elongation at 72 °C for 30 s. Fluorescence data were acquired after 10 s at 80 °C.

After the cycling program, melting curve analysis was performed by cooling to 40 °C for 2 min and then increasing the temperature to 95 °C with a slope of 0.2 °C/s while measuring the fluorescence continuously. The melting peak was obtained by plotting the negative first derivative of fluorescence against temperature. The threshold cycle (crossing point), in which the fluorescence significantly exceeds background, was determined by the LightCycler™ quantification software. Amplification efficiencies (slope) were calculated by a four-parameter sigmoidal fit *(20)* or, if not applicable, the "window-of-linearity" method *(21)*. Fold differences were calculated by a mathematical model described elsewhere *(22)*. All PCRs were conducted with six replicates. Statistical probabilities were determined by ANOVA and two-tailed *t*-statistics. All values presented are mean and SD.

The murine oxytocin mRNA (mOT-R) was chosen as a particular template possessing regions with a very high GC content and stable predicted secondary structures even at PCR elongation temperatures. A region within this template with a GC content of 85% was used as the experimental model. Trehalose enhances the amplification of mOT-R (Fig. 1), with increasing amounts of trehalose lowering the crossing point. Even at high cycle numbers, product yield was low without trehalose, but it was increased significantly in a concentration-dependent fashion by trehalose up to a concentration of 0.4 mol/L. The gain in amplicon amount was 202-fold when we compared "no trehalose", with an efficiency of 1.46 (SD, 0.12), with 0.2 mol/L trehalose, which had an efficiency of 1.95 (SD, 0.19) and a cycle difference of 7.95 (SD, 0.52) cycles compared with no trehalose. At 0.6 mol/L, we observed a decrease in amplification efficiency, but this was based on the significant decrease in the primer melting temperature at this high concentration (data not shown). This effect can be circumvented by lowering the primer annealing temperature according to Table 1.

We consider the optimal concentration of trehalose to

Table 1. Melting points of the GC-rich mOT-R and the less GC-rich S27a PCR products in the presence of trehalose and betaine.[a]

	Melting temperature, °C	
Concentration	**mOT-R**	**S27a**
Control	94.15 (0.24)	86.03 (0.07)
Trehalose, mol/L		
0.1	93.81 (0.36)	85.50 (0.12)
0.2	93.05 (0.26)	85.06 (0.18)
0.4	92.66 (0.71)	84.78 (0.21)
0.6	91.72 (0.53)	83.05 (0.07)
Betaine, mol/L		
0.2	93.42 (0.09)	85.78 (0.35)
0.5	94.25 (0.13)	85.91 (0.27)
1.0	93.28 (0.14)	84.68 (0.19)
2.0	89.79 (0.24)	81.07 (0.21)

[a] Results are means (SD) of six replicates.

be 0.2 mol/L, a concentration at which the amplification of the GC-rich mOT-R significantly ($P < 0.0002$) gains efficiency and primer annealing temperatures do not have to be adjusted. Betaine at 1 mol/L also significantly increased PCR efficiency (Fig. 1). At 2 mol/L, we encountered a significant decrease in amplification efficiency, suggesting that betaine concentrations must be adjusted more carefully than do trehalose concentrations.

A melting program was run to verify the presence of only one PCR product. The resulting melting curves verified this by having only one melting peak, but additionally we observed a decrease in the melting point in correlation to the trehalose concentration for both templates (Table 1). The DNA melting temperatures for mOT-R and S27a amplicons decreased by 0.5–1 °C for each 0.1 mol/L of trehalose. Betaine, already described as lowering the DNA melting temperature *(23)*, also exhibited this characteristic on both amplicons, but only at concentrations >1 mol/L.

To elucidate the possible thermostabilizing effect of trehalose on the *Taq* polymerase, we incubated the enzyme at 95 °C for 30 and 90 min before using it in a S27a amplification. The incubation was conducted in the standard PCR buffer to ensure the same environment as in a typical amplification with template. When we used the thermally "stressed" *Taq* polymerase that had been incubated in the presence of trehalose (0.2 mol/L) in a subsequent PCR reaction, we observed a weak thermostabilizing effect after a preincubation of 30 min (Fig. 1, inset). Amplification efficiencies were similar for *Taq* polymerase in the presence of trehalose (1.83; SD, 0.04) and in its absence (1.79; SD, 0.05). After 90 min of thermal preincubation in the absence of trehalose, a strong reduction in PCR efficiency was observed (1.57; SD, 0.16), which gave a relatively shallow amplification profile and low product yield after 35 cycles. Furthermore, the variation among the replicate samples was much higher. When the incubation was in the presence of 0.2 mol/L trehalose, the efficiency was lower than that for 30 min but significantly higher than at 90 min without trehalose (1.70; SD, 0.03). The variation among the replicates was also decreased compared with the latter conditions. Preincubation in the presence of 1.2 mol/L betaine also had a thermostabilizing effect compared with the control, but to a lesser degree than with trehalose, giving a lower PCR efficiency (1.67; SD, 0.08) and a higher crossing point.

For the exceptionally GC-rich oxytocin receptor, 35 cycles of amplification are needed to obtain a reasonable amount of PCR product, and the exponential phase of the amplification still exceeds this cycle number *(24)*. The addition of increasing amounts of trehalose in the PCR cocktail strongly enhanced the PCR efficiency of the mOT-R, providing the desired amplicon amounts at much lower cycle numbers. Only at the highest concentration of trehalose (0.6 mol/L) did we observe a slight decrease in PCR efficiency, but this effect was based on the reduction of the primer annealing temperature, which must be adjusted accordingly at this concentration (data not shown). We and our coworkers have successfully used this compound with several templates with low amplification efficiency. For single PCR amplifications with GC-rich templates, it seems feasible to use high concentrations of trehalose to increase the PCR efficiency. If multiplex PCRs are run, or when a PCR master mixture is used with templates of varying GC content, a concentration of 0.2 mol/L, which does not affect the PCR efficiency of templates with a low GC content, is suggested.

The DNA destabilization by trehalose that we describe here might have two different effects that enhance PCR: (*a*) the overall lowering of the template melting temperature, which supports the single-stranded state in which the polymerase elongation can take place; and (*b*) the elimination of secondary structures that still persist in single-stranded state and can, in addition to a complete stop of the elongation step *(10)*, lead to template switching of the *Taq* polymerase, mimicking splice variants because of small deletions *(25)*.

Rendering several enzymes more resistant to thermal stress in the presence of trehalose, thereby maintaining or even increasing their enzymatic activity, has been described for MMLV reverse transcriptase, restriction enzymes, and low-temperature polymerases *(7)*. Although trehalose renders *Taq* polymerase more stable when freezing PCR master mixtures *(26)*, data supporting a high-temperature thermostabilizing effect of trehalose on thermostable polymerases used for PCR amplification have been missing. In the presence of trehalose, we observed a significant thermostabilizing effect, so that after 90 min of preincubation at 95 °C, the enzyme retained nearly all of its enzymatic activity compared with unstressed fresh enzyme. This also occurs, but to a lesser extent, with betaine, which has been described to enhance the PCR amplification of GC-rich templates *(15, 17)*. This compound is routinely used at concentrations of 1–2 mol/L, which are much lower than the isostabilizing concentration of 5.2 mol/L *(23)*. Therefore, it has been debated that the DNA-helix-destabilizing action of betaine alone cannot account solely for the PCR-enhancing effect *(27, 28)*. The described ability of betaine to thermostabilize *Taq* polymerase might be the additional factor conferring the enhancing property.

In conclusion, trehalose is a compatible solute that greatly facilitates the PCR of GC-rich templates by reducing the DNA melting temperature and thermostabilizing the *Taq* polymerase. It thus could potentially be useful in the PCR amplification of difficult templates.

We thank D. Resuehr for fruitful discussions and the University Hospital of Hamburg (UKE) for providing excellent research facilities.

References

1. Singer MA, Lindquist S. Thermotolerance in *Saccharomyces cerevisiae*: the Yin and Yang of trehalose. Trends Biotechnol 1998;16:460–8.
2. Sleator RD, Hill C. Bacterial osmoadaptation: the role of osmolytes in bacterial stress and virulence. FEMS Microbiol Rev 2002;26:49–71.
3. Rajendrakumar CS, Suryanarayana T, Reddy AR. DNA helix destabilization by proline and betaine: possible role in the salinity tolerance process. FEBS Lett 1997;410:201–5.

4. Loos H, Kramer R, Sahm H, Sprenger GA. Sorbitol promotes growth of *Zymomonas mobilis* in environments with high concentrations of sugar: evidence for a physiological function of glucose-fructose oxidoreductase in osmoprotection. J Bacteriol 1994;176:7688–93.
5. Pflughoeft KJ, Kierek K, Watnick PI. Role of ectoine in *Vibrio cholerae* osmoadaptation. Appl Environ Microbiol 2003;69:5919–27.
6. Elbein AD, Pan YT, Pastuszak I, Carroll D. New insights on trehalose: a multifunctional molecule. Glycobiology 2003;13:17–27.
7. Carninci P, Nishiyama Y, Westover A, Itoh M, Nagaoka S, Sasaki N, et al. Thermostabilization and thermoactivation of thermolabile enzymes by trehalose and its application for the synthesis of full length cDNA. Proc Natl Acad Sci U S A 1998;95:520–4.
8. Spiess AN, Ivell R. A highly efficient method for long-chain cDNA synthesis using trehalose and betaine. Anal Biochem 2002;301:168–74.
9. Mizuno Y, Carninci P, Okazaki Y, Tateno M, Kawai J, Amanuma H, et al. Increased specificity of reverse transcription priming by trehalose and oligo-blockers allows high-efficiency window separation of mRNA display. Nucleic Acids Res 1999;27:1345–9.
10. McDowell DG, Burns NA, Parkes HC. Localised sequence regions possessing high melting temperatures prevent the amplification of a DNA mimic in competitive PCR. Nucleic Acids Res 1998;26:3340–7.
11. Varadaraj K, Skinner DM. Denaturants or cosolvents improve the specificity of PCR amplification of a G + C-rich DNA using genetically engineered DNA polymerases. Gene 1994;140:1–5.
12. Chakrabarti R, Schutt CE. Novel sulfoxides facilitate GC-rich template amplification. Biotechniques 2002;32:866–74.
13. Sarkar G, Kapelner S, Sommer SS. Formamide can dramatically improve the specificity of PCR. Nucleic Acids Res 1990;18:7465.
14. Demeke T, Adams RP. The effects of plant polysaccharides and buffer additives on PCR. Biotechniques 1992;12:332–4.
15. Baskaran N, Kandpal RP, Bhargava AK, Glynn MW, Bale A, Weissman SM. Uniform amplification of a mixture of deoxyribonucleic acids with varying GC content. Genome Res 1996;6:633–8.
16. Weissensteiner T, Lanchbury JS. Strategy for controlling preferential amplification and avoiding false negatives in PCR typing. Biotechniques 1996; 21:1102–8.
17. Henke W, Herdel K, Jung K, Schnorr D, Loening SA. Betaine improves the PCR amplification of GC-rich DNA sequences. Nucleic Acids Res 1997;25: 3957–8.
18. Frackman S, Kobs G, Simpson D, Storts D. Betaine and DMSO: enhancing agents for PCR. Promega Notes 1998;65:27.
19. Spiess AN, Walther N, Muller N, Balvers M, Hansis C, Ivell R. SPEER—a new family of testis-specific genes from the mouse. Biol Reprod 2003;68:2044–54.
20. Liu W, Saint DA. Validation of a quantitative method for real time PCR kinetics. Biochem Biophys Res Commun 2002;294:347–53.
21. Ramakers C, Ruijter JM, Deprez RH, Moorman AF. Assumption-free analysis of quantitative real-time polymerase chain reaction (PCR) data. Neurosci Lett 2003;339:62–6.
22. Pfaffl MW. A new mathematical model for relative quantification in real-time RT-PCR. Nucleic Acids Res 2001;29:e45.
23. Rees WA, Yager TD, Korte J, von Hippel PH. Betaine can eliminate the base pair composition dependence of DNA melting. Biochemistry 1993;32:137–44.
24. Breton C, Pechoux C, Morel G, Zingg HH. Oxytocin receptor messenger ribonucleic acid: characterization, regulation, and cellular localization in the rat pituitary gland. Endocrinology 1995;136:2928–36.
25. Viswanathan VK, Krcmarik K, Cianciotto NP. Template secondary structure promotes polymerase jumping during PCR amplification. Biotechniques 1999;27:508–11.
26. Klatser PR, Kuijper S, van Ingen CW, Kolk AH. Stabilized, freeze-dried PCR mix for detection of mycobacteria. J Clin Microbiol 1998;36:1798–800.
27. Weissensteiner T. Prostate cancer cells show a nearly 100-fold increase in the expression of the longer of two alternatively spliced mRNAs of the prostate-specific membrane antigen (PSM). Nucleic Acids Res 1998;26: 687.
28. Henke W, Loening SA. Recently, betaine has been introduced as an additive in different PCR strategies. Nucleic Acids Res 1998;26:687.

DOI: 10.1373/clinchem.2004.031336

Mass Spectrometry-Validated HPLC Method for Urinary Nitrate, *Dimitrios Tsikas* (Institute of Clinical Pharmacology, Hannover Medical School, Carl-Neuberg-Strasse 1, 30625 Hannover, Germany; fax 49-511-5322750, e-mail tsikas.dimitros@mh-hannover.de)

The L-arginine/NO biosynthetic pathway is involved in many physiologic and pathologic processes, including vasodilation and inhibition of platelet aggregation and adhesion. Nitrate (NO_3^-) and nitrite (NO_2^-) are the most abundant circulating and excretory NO metabolites in humans. In humans on a standardized low nitrate/nitrite diet, circulating nitrite reflects constitutive NO synthase activity *(1)*, whereas measurement of nitrate in urine is a reliable noninvasive method to assess whole-body NO synthesis in humans *(2)*.

Current analytical methods for the measurement of nitrate and nitrite include spectrophotometry, chemiluminescence, capillary electrophoresis, assays based on the Griess reaction, HPLC, and gas chromatography–mass spectrometry (GC-MS) *(3)*. Among these assays, GC-MS methods form the basis for reference methods *(4)*. Numerous HPLC methods using ultraviolet, electrochemical, or fluorescence detection have been reported for the analysis of nitrate and nitrite *(3)*. The majority of them, however, have not been validated against MS, and they are mostly limited to human plasma *(5)* or rat urine *(6)*. Recently, a commercially available HPLC-Griess system has been used for the analysis of urinary nitrite/nitrate in humans *(7)*, but it has not been externally validated, and analysis of nitrate requires its reduction to nitrite.

Here I report on a simple, rapid, GC-MS-validated anion-pairing HPLC method with ultraviolet absorbance detection at 205 nm for the accurate measurement of nitrate in human urine without sample pretreatment other than dilution of samples with the mobile phase. This HPLC method is not suitable to measure nitrate in human plasma.

HPLC analyses were performed with a Pharmacia LKB pump Model 2248 and an analytical column [250 × 4 mm (i.d.)] packed with Nucleosil 100–5C_{18} AB (Macherey-Nagel). The mobile phase consisted of water–acetonitrile (90:10 by volume) contained 10 mmol/L tetrabutylammoniumhydrogen sulfate (Merck), which serves as the anion-pairing agent. The pH of the mobile phase was adjusted to 8.4 by addition of sodium dihydrogen phosphate and 10 mol/L NaOH, and the flow rate was 1 mL/min. The variable ultraviolet–visible detector (Model Spectroflow 783; Kratos Analytical) was set at 205 nm. Analyses were performed at ambient temperature (22–26 °C). Sodium nitrate (purity >99.5%) and sodium nitrite (purity >99%) were purchased from Riedel-de Haën. Stock solutions of nitrate (80 mmol/L) and nitrite (10 mmol/L) were prepared in distilled water and diluted as appropriate with the mobile phase.

Mixtures of synthetic nitrate and nitrite containing these compounds at a constant molar ratio of 8:1 in the ranges 0–8000 μmol/L for nitrate and 0–1000 μmol/L for nitrite were used to prepare calibration curves. The reten-